Phase separation in solid ^{3}He-^{4}He mixtures: Comparison with theory of homogeneous nucleation

A. Smith
Millikelvin Laboratory, Royal Holloway University of London, Egham, Surrey, TW20 0EX, United Kingdom

V. A. Maidanov, E. Ya. Rudavskii, and V. N. Grigor'ev
Verkin Institute for Low Temperature Physics, 47 Lenin Avenue, Kharkov, 61103, Ukraine

V. V. Slezov
Kharkov Institute for Physics and Technology, National Science Centre, Kharkov, 61103, Ukraine

M. Poole, J. Saunders, and B. Cowan
Millikelvin Laboratory, Royal Holloway University of London, Egham, Surrey, TW20 0EX, United Kingdom
(Received 23 December 2002; published 17 June 2003)

NMR and pressure have been measured in a solid ^{3}He-^{4}He mixture as the temperature was lowered in steps through phase separation. The spin-echo method was used to detect the behavior typical for bounded diffusion and to estimate the diffusion coefficient, size and cluster concentration in the ^{3}He-enriched phase. The characteristic phase separation time constant of the mixture was found to decrease at lower temperatures. The results convincingly support homogeneous nucleation. From a comparison with theory, the surface tension at the boundary of the phase-separated clusters is found either from the cluster concentration, determined by NMR, or from the separation time constant, determined by pressure measurements. The results of the two independent determinations agree well and yield a surface tension coefficient of 1.27×10^{-2} erg/cm^2 (1.27×10^{-5} J/m^2).

DOI: 10.1103/PhysRevB.67.245314 PACS number(s): 67.80.Jd, 68.35.Rh

I. INTRODUCTION

The kinetics of phase transitions is one of the fundamental problems in condensed matter physics. It has been investigated theoretically and experimentally for many decades but some of its aspects are still unclear. It has been emphasized frequently in the literature[1–4] that helium and its isotopic mixtures hold much promise as model systems for studying phase transitions. However, these types of experiments and comparison with theoretical calculation are hampered by some difficulties. One of these is the realization of the conditions for homogeneous nucleation. There was a well-grounded hope for homogeneous nucleation in dilute liquid ^{3}He-^{4}He mixtures.[1] Numerous experimental attempts however failed to yield unambiguous results; rather, they detected heterogeneous nucleation which may be connected with vortex formation.[5,6]

In the case of solid helium, this problem might be solved provided that high-quality impurity-free samples are available. The quantum character of the diffusion processes in helium ensures fairly high diffusion coefficients, favouring the performance of experiments within reasonable times. We must emphasize the essential difference in the nucleation process in liquid and solid ^{3}He-^{4}He mixtures. In the first case it is impossible to attain a large supersaturation during cooling because of the terminal solubility of ^{3}He as $T\rightarrow0$. For solid mixtures there is no such limitation because the equilibrium concentration approaches zero as the temperature tends to zero. In this case we can achieve a large nucleation rate and the degree of supersaturation can thus be varied over a wide range. This makes the realization of homogeneous nucleation much easier.

Considerable attention has focussed recently on phase separation in solid ^{3}He-^{4}He mixtures.[3,4,7–13] In particular, the evidence of homogeneous nucleation was obtained for the first time,[3] where experimental results have been successfully compared with the Slezov-Schmeltzer theory.[14] This permitted estimation of the most important parameter responsible for nucleation—the surface tension σ at the new-phase cluster boundary, found from the pressure-time variation during the phase transition. In the work of Cowan and co-workers[4,11] the separation of a mixture has been studied by measuring the pressure and NMR simultaneously. Such measurements can provide additional evidence of homogeneous nucleation in solid ^{3}He-^{4}He mixtures, and permit estimation of σ, within a single experiment, from two independently measured quantities—the cluster size and the characteristic separation time constant, and thus improve the reliability of this very important parameter.

This work is devoted to the realization of such a possibility. Section II presents the basic theoretical relations that, according to Slezov and Schmeltzer,[14] describe homogeneous nucleation (Sec. II A) as well as a brief summary of bounded diffusion in the NMR experiments (Sec. II B); these are necessary for interpreting the experimental data. The experimental cell and techniques are described in Sec. III. The results are presented in Sec. IV together with a discussion, within the framework of the theory of homogeneous nucleation.

II. THEORY

A. Homogeneous nucleation in mixtures—cluster concentration and phase separation time constant

As mentioned above, simultaneous measurement of pressure and NMR during the process of phase separation of a

solid mixture permits us to obtain two very important parameters of the kinetics of nucleation—the concentration of the clusters and the time constant of the diffusion growth of these clusters. On the other hand, these parameters can be calculated within the homogeneous nucleation model.

Homogeneous nucleation in a uniform supersaturated mixture proceeds through the formation of clusters of the new phase at random sites. If the number of particles in a cluster, n, is smaller than a certain critical value n_c, controlled by the competition between the bulk and surface contributions to the thermodynamic potential, such a cluster is unstable and it vanishes. When $n>n_c$ the cluster grows. For a spherical cluster in a dilute binary mixture n_c is given by

$$n_c=\left(\frac{\beta}{\ln\frac{c_0}{c_f}}\right)^3, \tag{1}$$

where c_0 is the initial ^{3}He concentration of the mixture—the concentration before the supersaturation step, c_f is the equilibrium ^{3}He concentration of the matrix at the cluster boundary at the temperature T_f—after the supersaturation step and

$$\beta=\frac{8\pi}{3}\frac{\sigma a^2}{T_f}, \tag{2}$$

where a is the atomic distance, which is determined by $4\pi a^3/3=V_m/N_A$ where V_m is the molar volume and N_A Avogadro's number.

Both nucleation and the subsequent growth of the clusters are dependent on the quantity $I(n)$ characterizing the nucleation rate. $I(n)$ is a flow, which is determined by the particle number n in the space of cluster sizes. It is a very sharp exponential function of the number of particles, and $I(n_c)\equiv I_0$ which is the flow of the particles in the new phase through a critical point in the space of sizes, is of fundamental importance in all calculations. It can be written as[14,15]

$$I_0=\left(\frac{3\beta}{2\pi}\right)^{1/2}c_0^2\exp\left[-\frac{\Delta\Phi(n_c)}{T}\right], \tag{3}$$

where $\Delta\Phi(n)$ is the change in the thermodynamic potential when n particles of the initial mixture transform into a cluster. In the approximation considered

$$\Delta\Phi(n)=n\Delta\mu+4\pi a^2\sigma n^{2/3}, \tag{4}$$

and the difference between the chemical potentials is

$$\Delta\mu=T\ln\frac{c_f}{c_0}. \tag{5}$$

Using Eqs. (1), (2), and (5), we obtain

$$I_0=\left(\frac{3\beta}{2\pi}\right)^{1/2}c_0^2\exp\left(-\frac{\beta^3}{2\ln^2(c_0/c_f)}\right); \tag{6}$$

I_0 is strongly dependent on supersaturation of the metastable mixture. Assuming $c(T)=\exp(-Q/T)$ (quite a good approximation for dilute ^{3}He-^{4}He mixtures) we can obtain

$$I_0=c_0^2\left(\frac{3\beta}{2\pi}\right)^{1/2}\exp\left[-\frac{\beta_0^3}{2}\left(\frac{T_0}{Q}\right)^2\frac{1}{x(1-x)^2}\right], \tag{7}$$

where $x=T/T_0$ (T_0 is the phase separation temperature of the mixture), $\beta_0\equiv\beta(T_0)$ and Q is the effective heat of separation.

Although I_0 is finite for all x different from 0 and 1, Eq. (7) suggests that for practically any β_0 there is a region of supercooling where I_0, characterizing the nucleation rate, starts changing by orders of magnitude under very slight variation of x. As a result, nucleation is only observable in a narrow range of supersaturation; the process is unobservably slow at low degrees of supersaturation and practically instantaneous when the degree of supersaturation is high. This behavior permits us to introduce the concept of the highest cluster concentration N_m which corresponds to the end of nucleation at a pre-assigned temperature and at the initial supersaturation, when $(\Delta c/c)n_c\approx 1$. The relative cluster concentration per lattice site corresponding to this condition is[14]

$$N_m=(4c_0)^{1/4}\left(\frac{I_0}{\beta}\right)^{3/4}. \tag{8}$$

N_m is also responsible for the kinetics of the subsequent diffusion growth of the nascent clusters. Slezov *et al.*[14] estimate the characteristic time of the cluster growth up to coalescence (Ostwald ripening) to be

$$\tau_D=\frac{a^2}{3D}c_0^{-1/3}N_m^{-2/3}\approx\frac{a^2}{3D}\left(\frac{\beta}{c_0^2}\right)I_0^{-1/2}, \tag{9}$$

where D is the diffusion coefficient of ^{3}He in the separating mixture. (Note that the corresponding equations for N_m and τ in Ref. 14 contain typographical errors.)

According to Eq. (8), N_m is dependent on only one unknown parameter σ in I_0 and β. As soon as we know the cluster concentration, the interfacial surface tension coefficient can be estimated readily.

B. Spin echoes in restricted geometry and cluster sizes

The key experimental result of this study is the determination of the size of the new phase clusters created upon phase separation. It is this parameter that permits us to find the concentration of clusters N_m (calculated in the previous section) from particle conservation. In this work the size of the droplets was estimated by the pulsed NMR (spin echo) method.

In separated dilute mixtures the NMR transverse relaxation is influenced by the small size of the new phase droplets. This is most evident when diffusion is measured by the spin echo method, where the spin diffusion coefficient is found from the echo signal of the sample placed in a magnetic field with a gradient G after applying two or more resonant rf pulses separated by an interval t. With a conventional spin-echo pulse train $90°-t^*-180°$, the amplitude of the echo signal occurring at time $2t^*$ in a bulk sample can be expressed as

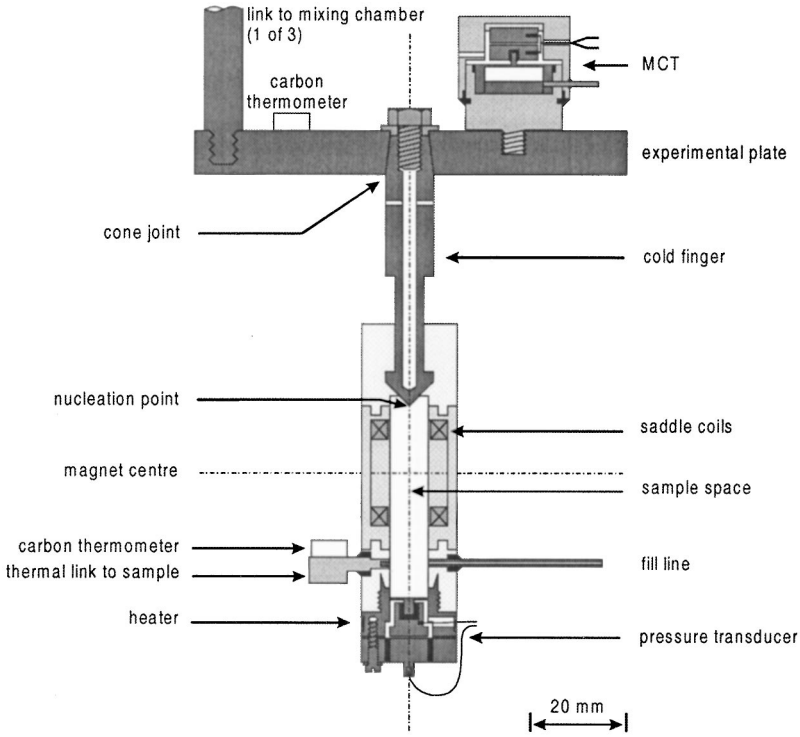

FIG. 1. Schematic view of the experimental cell.

$$E(2t^*)=\exp\left(-\frac{2}{3}\gamma^2G^2Dt^{*3}\right), \tag{10}$$

where γ is the gyromagnetic ratio.

If, however, the sample size d is smaller than the spin diffusion length $\sqrt{Dt^*}$, the dependence $E(t)$ becomes more complicated because the motion is bounded. The description of this effect[16,17] resulted in inconveniently lengthy formulas, difficult to use for processing experimental results. However simplification is possible through the use of an approximate model. It is evident that, so far as NMR is concerned, bounded diffusion in a field gradient is equivalent to unbound diffusion in a triangular field profile, the half-wavelength dimension being d. If the triangular profile is now approximated by a sinusoidal variation then we obtain a relatively simple expression for $E(t)$:

$$E(2t^*)=\exp\left\{-\frac{d^2\gamma^2G^2}{\pi^2}\tau_c^2\left[\frac{2t^*}{\tau_c}+4\exp\left(-\frac{t^*}{\tau_c}\right)-\exp\left(-\frac{2t^*}{\tau_c}\right)-3\right]\right\}, \tag{11}$$

where $\tau_c=d^2/\pi^2D$. We have determined, using numerical simulations, that Eq. (11) gives results in good agreement with the exact expression for a spherical droplet.[16] It is thus evident that through comparison of Eq. (11) with experimental data, we can find both the diffusion coefficient and the cluster size from this expression.

III. EXPERIMENTAL DETAILS

The experimental cell is shown in Fig. 1. The cell is supported on a copper cold finger extending down from the experimental plate, which is in good thermal contact with the mixing chamber of a dilution refrigerator.

The cell is of modular design in three parts: the cold finger and top third of the cell, the NMR coils in the middle and the pressure gauge in the bottom third. The copper cold finger is machined to a sharp point to encourage nucleation of the crystal from the liquid mixture at this point.

The middle section had the NMR saddle coil cast into it. The coil former was machined from Stycast 1266, with the coil spaced 0.5 mm from the sample space itself to give a large filling factor. The saddle coil had a diameter of 10 mm, and it was 20 mm long; this aspect ratio optimises the field homogeneity.

The capacitance of the coaxial lines to the cell was 240 pF, so with the coil inductance of 90 μH (40 turns on each side using 0.2-mm-diameter copper wire) a resonant frequency of 1.083 MHz was obtained. This Larmor frequency permits good discrimination between the T_1 signals from the ^{3}He rich clusters and the dilute background. An extra capacitor of 20 pF was connected in parallel with the coil at low temperature and the final tuning was performed with a small variable capacitor at room temperature. Once the coil had been wound to the right parameters and tested at 4 K the rest of the section was cast around it. The coil had a Q of 24 at room temperature, increasing to 160 at 4 K.

The bottom section of the cell contained a pressure transducer of the Straty-Adams type. A beryllium copper piece made up the base of the cell, forming its bottom wall: a thin flexible membrane 0.4 mm thick with a diameter of 8 mm. The BeCu was hardened by baking it at 320 °C for 3 h in a vacuum. A polished copper piece was then epoxied to the membrane as one plate of the capacitor. The separation of the capacitor plates was adjusted by a mylar spacer.

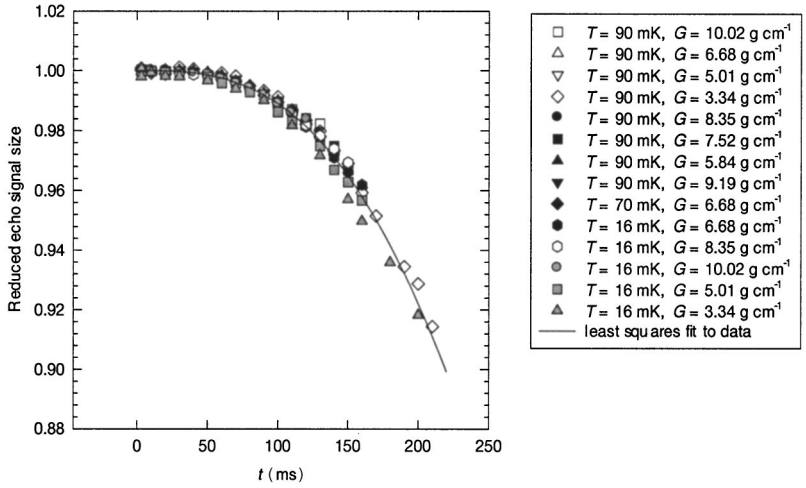

FIG. 2. Dependence of the reduced echo-signal amplitude on the interval between the pulses at different temperatures and magnetic field gradients. The curve is the least-squares approximation to the results by Eq. (11). Data are for temperatures between 90 and 16 mK and field gradients between 3.34 and 10.02 g cm^{-1}.

Thermometry was provided by two Speer carbon resistance thermometers calibrated using a ^{3}He melting curve thermometer and a germanium resistance thermometer (between 0.4 and 10 K). The sample mixture was made using standard volumetric techniques in a 50-l storage vessel using a digital pressure gauge with a resolution of 0.1 mbar. The ^{3}He came from a cylinder and the ^{4}He was added to make up the required concentration of $(1.00\pm0.01)\%$ from evaporated liquid. The crystal was grown by forcing the mixture into the cell at high pressure using a charcoal filled ''bomb'' in a ^{4}He transport Dewar.

In order to produce a sample with a minimum of defects the crystals were grown at constant pressure. The cold finger in the cell is cooled below the melting transition until solidification starts, indicated by a dropping pressure on the fill capillary. The nucleation point is then stabilized at this temperature and the other end of the cell is held just above the melting temperature. These conditions are maintained as the solid-liquid interface propagates through the cell. However, as the crystal grows the pressure in the cell drops, following the melting curve, so more liquid is forced in from the high pressure bomb. This process requires that the capillary is kept free of solid. The fill capillary enters the cell near the bottom and it is heat sunk at 4 K and on the 1-K pot. The pot was run at 2 K by partially constricting the pumping line. Below the 1-K pot the capillary comprised a 2-m length of CuNi tube which was thermally isolated all the way to the cell with two heaters wound onto it to keep it unblocked. Eventually no more liquid can be forced in as the crystal grows up into the fill capillary. At this point the heaters are turned off, the pot is pumped fully again and the pressure is increased on the capillary to make sure it stays plugged during the measurements. The NMR system was used to observe the crystal growth in the experimental cell. At 1 MHz the spin-lattice relaxation time T_1 of the ^{3}He in the liquid is significantly longer than that in the solid and a spin echo sequence was repeated every 5 seconds to keep the liquid signal saturated. Then, as the phase boundary moved through the coil, the echo could be seen to grow.

When the solidification was complete, the fill capillary heaters turned off and the 1-K pot run fully, the refrigerator circulation was stopped and the mixing chamber temperature regulated at 1.2 K for 180 h in order to anneal the crystal and reduce any inhomogeneities in ^{3}He concentration. Whilst annealing, the magnetization of the sample was continuously monitored and, in fact, no change was observed. The sample was then cooled to 500 mK to start measurements. The pressure $P_0=36$ bar was independent of temperature below 0.6 K.

The NMR measurements were all made using a home built coherent pulse spectrometer. The experimental procedure was as follows. The prepared and annealed sample was smoothly cooled to a temperature close to the separation temperature T_0 ($T_0=186$ mK for a 1% mixture). Then the temperature was lowered in steps and the pressure and the spin-echo signal were recorded. After the onset of phase separation, measurements were repeated at each step until equilibrium was established. In these experiments the diffusion in the ^{3}He nuclei was measured only at the lowest temperatures when nearly all ^{3}He was in the new-phase droplets. In later experiments we followed the diffusion coefficient and size of the droplets during the phase separation process.

IV. RESULTS AND DISCUSSION

A. Size and concentration of clusters

Figure 2 shows the reduced echo amplitude versus the interval between the rf pulses. The dependence was measured at different temperatures and magnetic field gradients after a chain of successive coolings of the sample. According to Eq. (11), the dependence is universal if the echo signals are raised to the power $(G_0/G)^2$ where G_0 is an (arbitrary) reference gradient. The data in Fig. 2 have been scaled in this way. The curve approximates Eq. (11), whose parameters were estimated by the least square method to give

$$D=(4.9\pm0.3)\times10^{-8}\ \text{cm}^2\,\text{s}^{-1} \quad \text{and} \quad d=4.5\pm0.5\ \mu\text{m}.$$

D agrees well with the spin diffusion coefficients for a bulk sample,[18–20] which suggests identical diffusion processes in ^{3}He clusters and in bulk ^{3}He.

TABLE I. Main characteristics of experiments upon step-by-step lowering of the sample temperature. The final concentration c_f is calculated by Edwards and Balibar's formula (Ref. 25).

No	T_f (mK)	c_f (%)	$\tau\times10^{-3}$ (s)	$D\times10^9$ (cm^2/s)	$\sigma\times10^2$ (erg/cm^2)	$N_m\times10^{15}$
1	183	0.91	76.50	0.17		
2	171	0.64	30.24	0.24	1.30	8.8
3	161	0.46	5.40	0.35	1.25	<0.1
4	150	0.31	4.32	0.55	1.24	0.3
5	140	0.20	3.78	0.88	1.24	<0.1
6	130	0.12	3.66	1.40	1.24	<0.1

The concentration of clusters can be found readily from their sizes. Since d is measured at quite low temperatures assuming that all ^{3}He is within the clusters, we obtain from the conservation of particles

$$\frac{\pi d^3}{6}\frac{N_A}{V_m}N_m=c_0 \quad \text{and} \quad N_m=3.2\times10^{-24}\times\frac{V_m}{d^3}c_0, \tag{12}$$

where N_A is Avogadro's number. Inserting these parameters, we obtain $N_m=(8.4\pm0.8)\times10^{-15}$. This result can be compared with Eq. (8) to estimate σ.

Before estimating σ from Eqs. (12) and (8), the following comments are appropriate.

(1) As mentioned in Sec. III the starting mixture for our sample contained 1% ^{3}He. It was also noted that the initial concentration can differ considerably from that in the crystal because of the isotope fractionation caused both by crystallization and by the desorption-induced increase in the pressure. In Refs. 3 and 13 the average concentration of the sample was refined by Mullin's formula[21] as a function of the pressure change ΔP_0 after complete separation of the mixture. In this case the inferred value of $c_0\approx1.7\%$ appears to be an overestimate. The overestimation may be attributed to the fact that at the end of crystallization the solid-liquid boundary moves below the filling capillary (see Fig. 1) and some of the liquid can still remain at the base of the cell. Some of this liquid is retained down to low temperatures, but under the influence of phase separation it vanishes. The fraction of the liquid, about 0.1–0.2%, is a sufficient reason for the explanation of the observed ΔP_0. Therefore, the initial ^{3}He concentration in the sample is somewhat uncertain. This, however, has no effect on the subsequent steps for which the initial and final concentration (c_i and c_f, respectively) are both determined by the phase diagram of the mixture. Possibilities for the refinement of c_0 are discussed below.

(2) The clusters of the new phase whose sizes we measure in the experiment developed after several successive stepwise coolings (some characteristics of the steps at which the changes in the concentration become measurable are shown in Table I and Fig. 3). Basically, new clusters can form at any step. Because of their low concentration at each step ($\sim10^{-15}$), we can assume that nucleation is an independent process and the experimental N_m found at low temperatures may be taken as a sum of contributions from all the previous steps.

(3) The equations in Sec. II A refer to the case when the mixture becomes separated completely after one cooling step. On a multistep cooling, the expression for the nth step can be derived rigorously by solving Eqs. (43) in Ref. 14 for different starting conditions, taking into account the previously formed clusters. However, since nucleation takes a shorter time than the diffusion growth and it proceeds independently (see above), the kinetics of the cluster growth may be thought of as invariable, and the refinement of Eq. (9) reduces to substitution of $c_0^{-1/3}$ with $(c_0-c_{fn})^{2/3}/c_{in}$ (c_{fn} and c_{in} are the final and initial concentrations at the nth step). In the expressions for β (and I_0) c_0 should also be replaced by c_{in}.

Taking into account these comments, we can obtain from Eq. (8) the total N_m value corresponding, within the error, to the experimental result 8.4×10^{-15} if we used $\sigma=1.27\times10^{-2}$ erg/cm^2. The value of N_m for each step is presented in Table I (column 7). It is seen that most clusters are formed at steps (2) and (4). In the calculation the number of clusters at step (1) was assumed to be negligible. This is true for $c_0\leqslant1.25\%$. The more prolonged separation time at step (1) supports this assumption.

B. Kinetics of phase separation

In the experiments we measured the change in the pressure of the sample after a step lowering of the temperature. As was noted in Sec. III, in a homogeneous sample the pres-

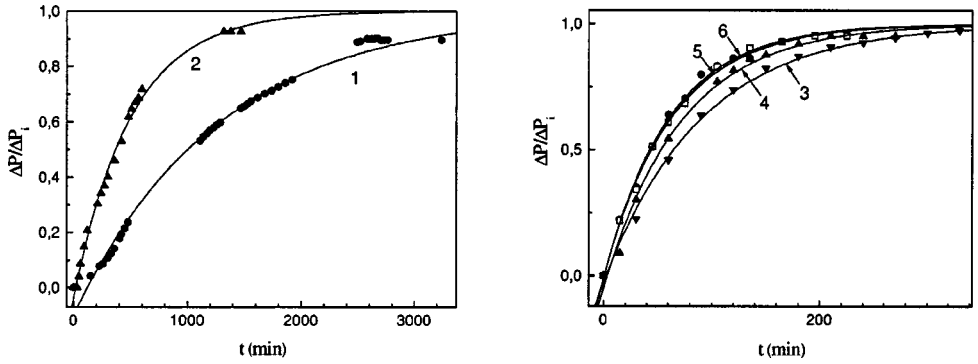

FIG. 3. Time dependence of the relative change in the sample pressure after a step lowering of temperature. The curves are least square approximations to Eq. (13). The curve numbers correspond to those of Table I.

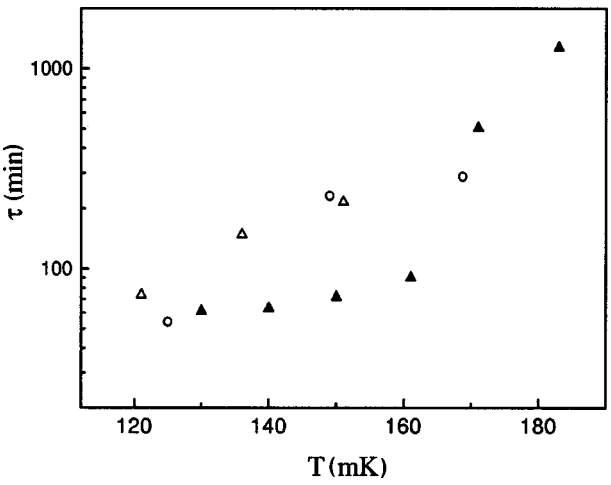

FIG. 4. Characteristic separation time versus temperature. Filled triangles—present work; open triangles—Ref. 13, $P_0=36$ bar; circles, Ref. 13 $P_0=35.7$ bar.

sure below 600 mK is unresponsive to the drop of the temperature. The first change in P was recorded when the temperature fell to 183 mK. At the previous step ($T_f=207$ mK), the pressure remained constant, to within the measurement accuracy, for several hours, but even in this case there were changes in the NMR signals. This is possible if the concentration is non-uniform (at 207 mK separation occurs only at $c_0 \geqslant 1.6\%$) and there is a some pressure gradient over the sample. The pressure was measured at 183 mK and lower T_f until it reached equilibrium.

In accordance with earlier experimental results (e.g., see Refs. 12 and 13), the pressure-time dependences in Fig. 3 can be approximated well by an exponential dependence of the type

$$P_f - P = (P_f - P_i)e^{-t/\tau}, \tag{13}$$

where P_i and P_f are the equilibrium pressures at the initial and final temperatures. The deduced values for τ decrease with lowering temperature (see Fig. 4); this is consistent qualitatively with previous work[8,12,13] for this temperature interval and may be attributed to the quantum diffusion coefficient which increases when the concentration of the mixture decreases. For comparison, Fig. 4 includes data from Ganshin *et al.*[13] for a mixture with $c_0 \approx 2\%$ and a similar value for P_0; the data agree qualitatively. The quantitative distinction may be caused by the different concentration of clusters in their work.

If (in accordance with Ganshin *et al.*[13]) we assume that the diffusive process through which the mixture separation occurs corresponds to spin diffusion, then the diffusion coefficient D in Eq. (9) can be calculated as[22,23]

$$D = \frac{D_0}{c}\left(1 - \frac{c}{c_c}\right)^{1.7}, \tag{14}$$

where D_0 is a constant, c_c is the critical concentration corresponding to the formation of an immobile macroscopic impurity cluster.[22] D_0 and c_c are functions of density. Using the parameters of Grigor'ev,[23] we obtain $D_0=2.4\times10^{-12}$ cm^2/s and $c_c=4.7\%$ for this sample. From these parameters, the diffusion coefficients were calculated for each step (Table I, column 4). The D values correspond to the average concentration for a particular step. The σ values (Table I, column 6) were calculated from Eq. (9) assuming that for a particular step τ is determined by the number of clusters formed at this and the previous steps. The σ values calculated at different steps are close and agree well with that found from the cluster concentration. It is clear that the degree of consistency of these data is mainly determined by the steepness of the function I_0 and is actually determined by the supersaturation interval within which the mixture is being separated. Nevertheless, we may assert that the good agreement with the Slezov-Schmeltzer theory[14] is evidence in favor of homogeneous nucleation in the solid ^{3}He-^{4}He mixture.

The deduced values for σ could be used to determine c_0 if we reverse Eq. (9) for step (1). This yields $c_0 \approx 1.2\%$, but its accuracy is open to question because nucleation, as in Penzev *et al.*,[3] can be heterogeneous at such small supersaturation. This assumption is supported by Fig. 4, where τ for step 1 is much smaller than the extrapolated data for the subsequent steps.

TABLE II. Comparison of the results on interfacial surface tension in phase separated ^{3}He-^{4}He mixtures in different experiments.

Coexisting phases	Basic parameters or dependences used to estimate σ	$\sigma\times10^2$ (erg/cm^2)	Reference
^{3}He-rich cluster–^{4}He matrix	Cluster concentration	1.27	This study
	Separation time	1.26	
^{4}He-rich cluster–^{3}He matrix	τ versus supersaturation	1.43[a]	3
^{4}He cluster around vacancy in ^{3}He matrix	Pressure variation during thermocycling	1.48[a]	24

[a]These values are corrected as compared with Refs. 3 and 24 because the definition of a differs from that in the theoretical consideration (Ref. 14).

C. Comparison with other experiments

It is worthwhile to compare the above results with those of other experiments on the kinetics of phase separation in solid ^{3}He-^{4}He mixtures. Recently experiments have been performed on dilute ^{4}He-^{3}He mixtures[3,24] where phase separation leads to the formation of nearly pure ^{4}He inclusions in the nearly pure ^{3}He matrix. The data obtained are summarized in Table II along with the results of this study.

In Penzev *et al.*[3] the kinetics of phase separation was investigated at different supercoolings of the mixture $\Delta T = T_i - T_f$, into the two-phase region. At low ΔT the separation time constant is, as expected, high and almost independent of T_f, which is due to heterogeneous nucleation. At high ΔT, τ is small and T_f-independent again, and τ increases sharply with growing T_f only in a narrow region of ΔT. This behavior is consistent with the theory of homogeneous nucleation. The σ data (interfacial surface tension) are presented in Table II.

Phase separation in dilute ^{4}He-^{3}He mixtures produces different systems.[24] Here temperature cycling of a two-phase crystal leads to the formation of a vacancy cluster in the region of separation, which consists of ordered ^{4}He atoms arranged around a vacancy. In this case the pressure variation in the crystal is determined by the change in the cluster radius, and we can thus estimate σ as a fitting parameter from experimental results (see Table II).

The interfacial surface tension coefficients of Penzev *et al.*[3] and Maidanov *et al.*[24] are in good agreement (Table II), and they exceed the σ of this study only by 15–20 %. If we take this distinction as real, it could be related to the difference in the cluster density between the ^{4}He or ^{3}He-enriched phases.

The similarity of the results supports the validity of the methods used. The calculated σ is about 1.6 times lower than the measured value for separated liquid mixtures.[26] It is possible that in this case the lower σ values are determined by the small sizes of the new phase clusters and the vacancy clusters.

V. CONCLUSION

Experiments on the kinetics of phase separation carried out on dilute mixtures of ^{3}He in ^{4}He and dilute mixtures of ^{4}He in ^{3}He show that the conditions for homogeneous nucleation can be realized in high-quality crystals (due to their growth at constant pressure or to thermocycling in the two-phase region). For the first time the main parameter of the theory, namely the interphase surface tension σ of the solid ^{3}He-^{4}He mixture, was obtained through two independent experiments—bounded diffusion measurements and measurements of the separation time constant. It was shown that their values obtained in different experiments within the homogeneous nucleation model are in good agreement. Realization of homogeneous nucleation in solid ^{3}He-^{4}He mixtures opens up new possibilities for the comprehensive quantitative correlation with theory.

[1] I.M. Lifshits, V.I. Polessky, and V.A. Khokhlov, Zh. Eksp. Teor. Fiz. **74**, 268 (1978) [Sov. Phys. JETP **47**, 137 (1978)].

[2] S. Balibar, T. Misusaki, and Y. Sasaki, J. Low Temp. Phys. **120**, 293 (2000).

[3] A. Penzev, A. Ganshin, V. Grigor'ev, V. Maidanov, E. Rudavskii, A. Rybalko, V. Slezov, and Ye. Syrnikov, J. Low Temp. Phys. **126**, 151 (2002).

[4] A. Smith, M. Poole, J. Saunders, and B. Cowan, J. Low Temp. Phys. (to be published).

[5] V. Chagovets, E. Rudavskii, G. Sheshin, and I. Usherov-Marshak, J. Low Temp. Phys. **113**, 1005 (1998).

[6] S. Burmistrov, V. Chagovets, L. Dubovskii, E. Rudavskii, T. Satoh, and G. Sheshin, Physica B **284–288**, 321 (2000).

[7] R. Shrenk, O. Friz, Y. Fujii, E. Syskakis, and F. Pobell, J. Low Temp. Phys. **84**, 133 (1991).

[8] V.A. Shvarts, N.P. Mikhin, E.Ya. Rudavskii, A.M. Usenko, Yu.A. Tokar, V.A. Mikheev, Fiz. Nizk. Temp. **21**, 717 (1995) [Low Temp. Phys. **21**, 556 (1995)].

[9] S.C.J. Kingsley, I. Kosarev, L. Roobol, V. Maidanov, J. Saunders, and B. Cowan, J. Low Temp. Phys. **110**, 400 (1998).

[10] P.R. Halley and E.D. Adams, J. Low Temp. Phys. **110**, 121 (1998).

[11] S.C.J. Kingsley, V. Maidanov, J. Saunders, and B. Cowan, J. Low Temp. Phys. **113**, 1017 (1998).

[12] A.N. Ganshin, V.N. Grigor'ev, V.A. Maidanov, N.F. Omelaenko, A.A. Penzev, E. Rudavskii, and A.S. Rybalko, Fiz. Nizk. Temp. **25**, 356 (1999) [Low Temp. Phys. **25**, 259 (1999)].

[13] A.N. Ganshin, V.N. Grigor'ev, V.A. Maidanov, N.F. Omelaenko, A.A. Penzev, E. Rudavskii, A.S. Rybalko, and Yu.A. Tokar, Fiz. Nizk. Temp. **25**, 796 (1999) [Low Temp. Phys. **25**, 592 (1999)].

[14] V.V. Slezov and J. Schmelzer, Fiz. Tverd. Tela, (Leningrad) **39**, 2210 (1997) [Phys. Solid State **39**, 1971 (1997)].

[15] V. Folmer, *Kinetik der Phasenbildung* (Steinkopf, Dresden, 1939).

[16] B. Robertson, Phys. Rev. **151**, 273 (1966).

[17] C.H. Neuman, J. Chem. Phys. **60**, 4508 (1974).

[18] R.C. Richardson, E. Hunt, and H. Meyer, Phys. Rev. **138**, A1326 (1965).

[19] B.N. Eselson, V.A. Mikheev, and V.N. Grigor'ev, Fiz. Nizk. Temp. **2**, 1229 (1976) [Sov. J. Low Temp. Phys. **2**, 599 (1976)].

[20] B. Cowan and M. Fardis, Phys. Rev. **44**, 4304 (1991).

[21] W.J. Mullin, Phys. Rev. Lett. **20**, 254 (1968).

[22] Yu.M. Kagan and L.A. Maksimov, Zh. Eksp. Teor. Fiz. **84**, 792 (1983) [Sov. Phys. JETP **57**, 459 (1983)].

[23] V.N. Grigor'ev, Fiz. Nizk. Temp. **23**, 5 (1997) [Low Temp. Phys. **23**, 3 (1997)].

[24] V. Maidanov, A. Ganshin, V. Grigor'ev, A. Penzev, E. Rudavskii, A. Rybalko, and Ye. Syrnikov, Pis'ma Zh. Eksp. Teor. Fiz. **73**, 329 (2001) [JETP Lett. **73**, 289 (2001)].

[25] D. O. Edwards and S. Balibar, Phys. Rev. B **39**, 4083 (1989).

[26] O. Ohishi, H. Yamamoto, and M. Suzuki, J. Low Temp. Phys. **112**, 199 (1998).